ChemComm

Ultrasensitive fluorescence detection of transcription factors based on kisscomplex formation and the T7 RNA polymerase amplification method†

Kai Zhang, ID* Ke Wang, Xue Zhu and Minhao Xie*

Herein, we report a kisscomplex based protein fluorescence assay (KPFA) method, which employed the formation of a kisscomplex and the T7 RNA polymerase amplification method, for the assay of transcription factors with high sensitivity.

Transcription factors (TFs) are a class of DNA-binding proteins that regulate a variety of essential cellular processes, such as genome replication, gene transcription, cell division and DNA repair through their binding and interaction with DNA. Therefore, owing to the pivotal role of TFs in the regulation of cell development, gene expression as well as its close relationship with human diseases, analyzing multiple TFs can provide more valuable information for understanding the mechanisms of cell development, differentiation, and growth in cellular processes. For this end, a broad class of methods that can simultaneously analyze multiple TFs has been developed for the detection of TFs.[1–6] Unfortunately, these strategies for assay TF concentration or binding activity are generally cumbersome. Therefore, the development of new methods for general, cost-effective, and sensitive detection of transcription factors is currently in great demand.

A riboswitch is a regulatory segment located in the 5′ untranslated region (UTR) of mRNA.[7–10] It can regulate gene expression by binding to a small metabolite.[11] In a typical riboswitch, there is an aptamer domain for binding the target and an expression domain. Recently, riboswitches have attracted great interest for many field studies. For example, a riboswitch leads to dimerization at the dimerization initiation site (DIS) of a loop–loop complex for the formation of a "kissing complex".[12,13] The "kissing complex" is formatted by the Watson–Crick pairing of a self-complementary sequence within an apical hairpin loop. Based on this, Toulmé *et al.* reported biosensors which are based on riboswitch kissing complexes for the detection of

small ligands.[14] We also reported kissing complex-induced strategies for the assay of adenosine, adenosine deaminase, DNA and RNA.[15,16] These new strategies are new concepts for biosensors and open opportunities for the design of more novel assay methods based on the kissing-complex-induced strategy. However, these methods are strictly based on the negative recognition element in the presence of a ligand which limits the field of application. To expand the application of riboswitches and to enrich the applied range of ELISA, it is desirable to engineer a riboswitch-based assay method and study the potential application of this method.

Enzyme-linked immunosorbent assay (ELISA) is a common assay for the detection of antigens in real samples, and it has been widely used in clinical diagnosis.[17–23] This method uses an enzyme, usually peroxidase, to catalyze the conversion of a substrate into a colored product for quantification.[24–29] Classical ELISA is a ligand-binding assay which requires the screening of a recognition unit (antibody) in *in vitro* assays and animal models. However, the cumbersome acquisition process of antibody selection reduces the practical applications of ELISA.[30–36] Also, the established ELISA was highly dependent on the sandwich structure of antibody–antigen–antibody. The formation of the structure may influence the native tertiary structure of the protein.[37–41] These limitations call for the development of a new protein assay methodology characterized by simplicity, sensitivity, and antibody-free.[42–44]

In the present work, we develop an ultrasensitive transcription factor detection method using the kisscomplex based protein fluorescence assay (KPFA) by integrating protein–DNA interaction, the advantage of aptakiss and isothermal exponential amplification in a one-pot reaction. We employed the microphthalmia-associated transcription factor (MITF), which is a kind of TF, as the model. In our strategy, the combination of the duplex DNA and TF can convert DNA1 from the "OFF-state" to the "ON-state", in which the aptakiss part of DNA1 is functional. The subsequent formation of the aptakiss complex with DNA2 builds a bridge which immobilizes DNA2 on the plate well surface. The immobilization of DNA2 triggers the amplification reaction and the recovery of the fluorescence which is detectable with the help of T7 RNA polymerase.

Key Laboratory of Nuclear Medicine, Ministry of Health, Jiangsu Key Laboratory of Molecular Nuclear Medicine, Jiangsu Institute of Nuclear Medicine, Wuxi, Jiangsu 214063, China. E-mail: zhangkai@jsinm.org, xieminhao@jsinm.org; Fax: +86-510-85508775; Tel: +86-510-85508775
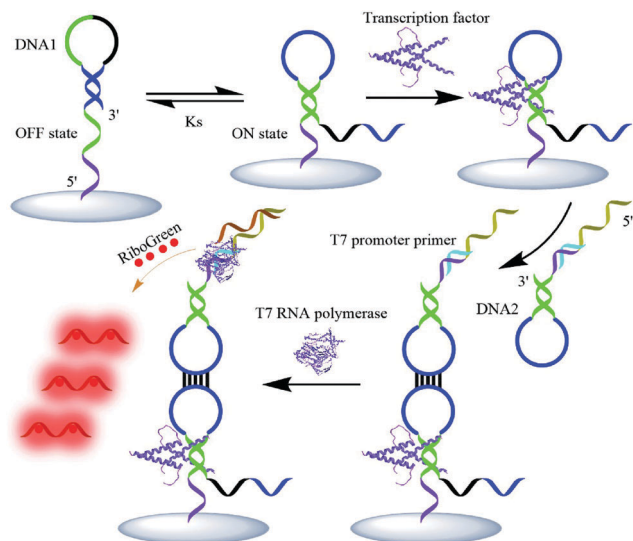
Scheme 1 Schematic diagram showing the principle of the kisscomplex based protein fluorescence assay (KPFA) for the detection of transcription factor.
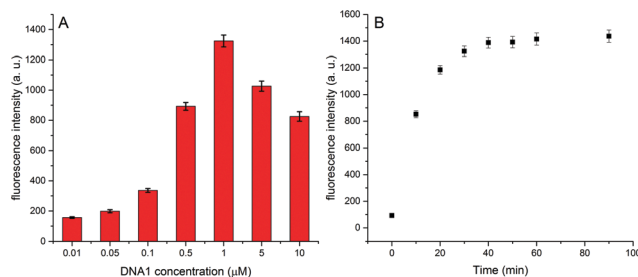

Fig. 1 (A) Fluorescence intensity at different concentrations of DNA1 under the conditions of 200 pM MITF, 1 μM DNA2/T7 promoter primer duplex and 60 units of T7 RNA Polymerase Plus; (B) fluorescence intensity versus time in the presence of 60 units of T7 RNA Polymerase Plus under the conditions of 1 μM DNA1, 200 pM MITF and 1 μM DNA2/T7 promoter primer duplex.

The method for the detection of MITF by the kisscomplex based protein fluorescence assay (KPFA) is depicted schematically in Scheme 1. DNA1 contains four functional domains: (i) a poly-A spacer is added between the amino-group and the hybridization part to link DNA1 to the plate well, (ii) a double-stranded MITF-binding domain (green sequence), (iii) a switch part for the formation of the kisscomplex (blue sequence between green parts), and (iv) a hybridization part (blue sequence at the 3′-end). DNA2 also contains four functional domains: (i) a kiss part for the formation of the kisscomplex (blue part), (ii) a double-stranded hybridization domain (green sequence), (iii) the sequence for the T7 RNA polymerase Plus upstream primer hybridization part (cyan sequence), which will hybridize with the T7 promoter primer duplex, and (iv) an amplification part (Kelly sequence at the 5′-end). The sequences are listed in Table S1 (ESI†). DNA1 was well designed in an equilibrium with two conformations: "OFF-state" and "ON state". At the "OFF-state", the switch part is hybridized with the hybridization part, which leads to the forbidding of the kisscomplex loop formation. The "ON-state" formation will expose the kisscomplex part which exists in a loop form. MITF binding shifts this equilibrium towards the "ON-state", activating the formation of the kisscomplex between DNA1 and DNA2. The space structures of DNA1 ("OFF state" and "ON state"), DNA2 and the kissing complex can be found in Fig. S1 (ESI†). Then the labeled DNA2/T7 promoter primer duplex will generate thousands of RNA. The binding of the added RiboGreen dyes to the RNA fragments will generate the fluorescence readout which reflects the dose of the MITF.

Several important aspects involved in the strategy were examined. First, we found that the DNA1 density packed on the surface cannot be too high, because it will reduce the binding efficiency between MITFs and DNA1. In our system, this may be caused by the steric hindrance effects of modified DNA1 on the MITFs. Therefore, we characterized the relationship between the probe modification density and the fluorescence signal intensity

in our experiments. As is shown in Fig. 1A, the maximum fluorescence signal intensity can be obtained at the DNA1 concentration of 1 μM. Therefore, the plate wells used in this work are all modified with 1 μM DNA1 solutions. From Fig. 1A we obtained that the fluorescence intensity increases with increasing the DNA1 concentration from 0.01 μM to 1 μM. However, a higher concentration of DNA1 cannot give a higher fluorescence intensity. This interesting phenomenon may be attributed to the modified DNA1 steric effect with MITF. Second, we checked the minimum reaction time of the MITFs combining with DNA1 by measuring the fluorescence signals in the absence of MITFs. As shown in Fig. 1B, the maximum fluorescence intensity was obtained at the incubation time of 30 min. So, 30 min is chosen for MITF incubation in this work.

Next, we added MITF to investigate the quantitative relationship of the strategy. The fluorescence signal intensity increased along with the concentration of MITF. The result obtained was reasonable because a higher concentration of MITF will convert more DNA1 to the "ON-state", making more functional DNA1 connected with DNA2 through the aptakiss part, further giving a higher fluorescence intensity. Fig. 2 shows the fluorescence intensity of the DNA1/MITF/DNA2 complex, which has been treated with different concentrations of MITF ranging from 0 to
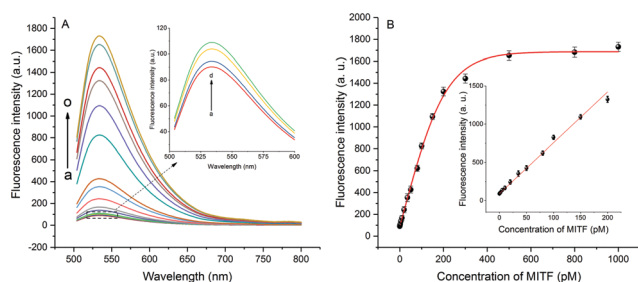

Fig. 2 (A) Fluorescence emission spectra at different MITF concentrations (0, 0.5, 1, 2, 5, 10, 20, 35, 50, 100, 150, 200, 300, 500, and 1000 pM (from a to o)). The inset shows the fluorescence emission of 0, 0.5, 1, and 2 pM MITF (from a to d). (B) Relationship between the fluorescence intensity and the concentration of MITF. The inset shows the linear relationship over the concentration range of 0–200 pM. All the data were obtained from three independent experiments and error bars denote standard deviations.

1000 pM. In order to show the relationship clearer, the fluorescence intensity of the DNA1/MITF/DNA2 complex *vs.* the logarithms of the concentration of MITF is also given in Fig. S2 (ESI†). A linear response of this sensor can be obtained in the range of 0–200 pM (inset in Fig. 2B) with a correlation equation of $Y = 90.66 + 6.65X$ ($R^2 = 0.9951$), where Y is the fluorescence intensity and X is the concentration of MITF (picomolar). The detection limit of 0.23 pM was obtained based on the 3σ method, which is lower than those of our previous reports based on the duplex-specific nuclease based method (1.1 pM)[6] and other previous reports (please see Table S2, ESI†). Such a significant improvement in the detection sensitivity might be attributed to the high specificity of MITF to DNA1, high recognition ability of the two parts of the kisscomplex to each other, and the high amplification efficiency of the T7 RNA polymerase.

The specificity of the sensing system is an important parameter for a method. An excellent detection method should not only possess good sensitivity but also have good specificity. The specificity of this assay was further investigated by adding transcription factor NF-κB p65, carcinoembryonic antigen (CEA), thrombin, TATA binding protein (TBP), and prostate specific antigen (PSA) with the same concentration (200 pM) in the reaction system, respectively, in which DNA1 containing a perfectly MITF-binding domain was adopted. As shown in Fig. 3, low fluorescence intensity was detected in the presence of NF-κB p65, CEA, thrombin, TBP, and PSA, which was slightly higher than that in the control experiment. The results demonstrated that this method has a specificity to discriminate target proteins.

The commonly used biosensors are usually inefficient when detecting proteins in complex biological samples, since the natural system contains ubiquitous endogenous components producing a high fluorescence background. To demonstrate the capability of the proposed method in real sample analysis, we perform the MITF assay using 10-fold diluted nuclear extract samples extracted from A549 cell lines. Table 1 shows the experimental results obtained in MITF-spiked nuclear extract samples
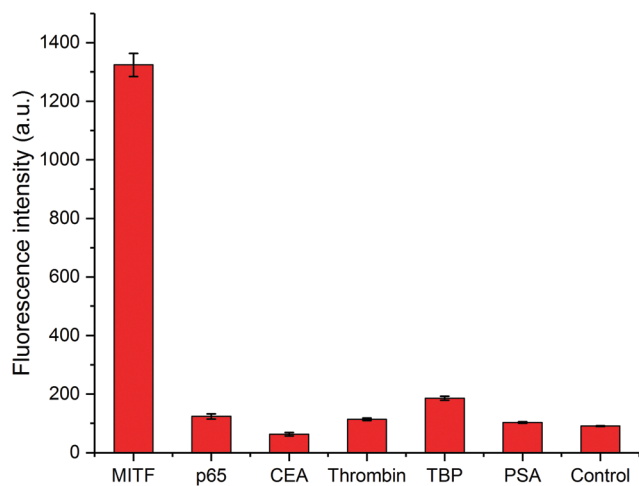
Table 1 Results of the recovery test of MITF in 10-fold diluted nuclear extracts

MITF			
Sample	Added (pM)	Found (pM)	Recovery (%)
1	0	45.68	
2	2	47.69	100.5 ± 2.8
3	5	50.42	94.8 ± 2.6
4	10	56.23	105.5 ± 3.5
5	20	67.59	109.6 ± 3.1
6	50	95.35	99.3 ± 2.8
7	100	150.68	105.0 ± 2.6

spiked with seven concentrations (0 pM, 2 pM, 5 pM, 10 pM, 20 pM, 50 pM, and 100 pM,). MITF concentration recoveries of values 94.8–109.6% were achieved. Therefore, the KPFA exhibits excellent potential to be applied in clinical tests.

To demonstrate the generality of our approach, we designed a method with just a little change in the sensing sequence of DNA1 (DNA3 in Table S1, ESI†), instead, for the assay of NF-κB p65 (p65), a TF present in virtually all eukaryotic cells. We explored the fluorescence emission spectra in the presence of different concentrations of NF-κB p65 (Fig. 4A). The results showed that as the NF-κB p65 concentration increased, the fluorescence intensity increased according. Fig. 4B shows the relationship between the fluorescence intensity and the NF-κB p65 concentration, and the inset shows the calibration curve for quantitative analysis of NF-κB p65. The intensity was linearly dependent on the concentration of NF-κB p65 over the range of 0–200 pM by using the equation $Y = 99.78 + 6.87X$ ($R^2 = 0.9934$), where Y is the fluorescence intensity and X is the concentration of NF-κB p65, and a detection limit of 0.496 pM could be obtained according to the responses of the blank tests plus 3 times the standard deviation (3σ). To test the specificity of this method, five proteins (MITF, CEA, thrombin, TBP, and PSA) with the same concentration (200 pM) were selected as the detection model. Fig. S3 (ESI†) shows the fluorescence changes for the target NF-κB p65 and other proteins. These results clearly demonstrate that the approach shows a high selectivity toward the target TF.

In summary, we have proposed a kisscomplex based protein fluorescence assay (KPFA) for TFs based on riboswitch and T7
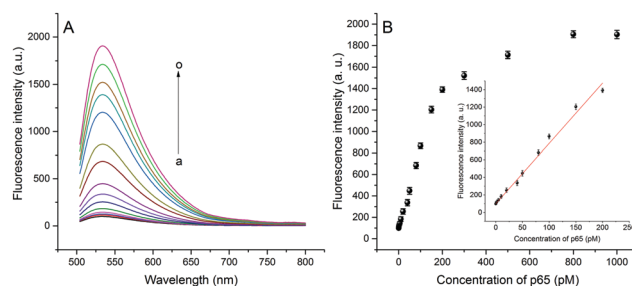

Fig. 3 Fluorescence intensity of the KPFA test of MITF and other proteins, showing the specificity of the assay. The concentrations of the proteins were all 200 pM.

Fig. 4 (A) Fluorescence emission spectra at different NF-κB p65 concentrations (0, 1, 2, 5, 10, 20, 40, 50, 80, 100, 150, 200, 300, 500, and 1000 pM (from a to o)). (B) Relationship between the fluorescence intensity and the concentration of NF-κB p65. The inset shows the linear relationship over the concentration range of 0–200 pM. All the data were obtained from three independent experiments and error bars denote standard deviations.

RNA polymerase amplifications. By taking advantage of the high amplification efficiency of T7 RNA polymerase, high sensitivities of MITF and NF-κB p65 are realized with detection limits as low as 0.23 pM and 0.496 pM, respectively, which are superior or comparable to those of the previous reports. Furthermore, this method has also demonstrated some other distinguishing features. First, this method makes use of the high affinity effect between protein and DNA interactions and is quite resistant to nonspecific proteins, thus resulting in high specificity in nuclear extracts. Second, the application of KPFA could be expanded, because many DNA duplexes have been found for combing with proteins. This method could be used for other protein assays by only changing the protein combing domain in DNA1. Therefore, this strategy holds great promise as a general and highly sensitive method for other protein detections and shows great potential for practical applications in transcription factor-based early stage cancer diagnosis.

Notes and references

1 A. Vallée-Bélisle, A. J. Bonham, N. O. Reich, F. Ricci and K. W. Plaxco, *J. Am. Chem. Soc.*, 2011, **133**, 13836–13839.
2 A. J. Bonham, K. Hsieh, B. S. Ferguson, A. Vallée-Bélisle, F. Ricci, H. T. Soh and K. W. Plaxco, *J. Am. Chem. Soc.*, 2012, **134**, 3346–3348.
3 Y. Zhang, J. Hu and C.-y. Zhang, *Anal. Chem.*, 2012, **84**, 9544–9549.
4 J. Yin, P. Gan, F. Zhou and J. Wang, *Anal. Chem.*, 2014, **86**, 2572–2579.
5 K. Zhang, K. Wang, X. Zhu and M. Xie, *Biosens. Bioelectron.*, 2016, **77**, 264–269.
6 K. Zhang, K. Wang, X. Zhu, M. Xie and X. Zhang, *Biosens. Bioelectron.*, 2017, **87**, 299–304.
7 S. K. Desai and J. P. Gallivan, *J. Am. Chem. Soc.*, 2004, **126**, 13247–13254.
8 S. D. Gilbert, C. E. Love, A. L. Edwards and R. T. Batey, *Biochemistry*, 2007, **46**, 13297–13309.
9 A. Haller, M. F. Soulière and R. Micura, *Acc. Chem. Res.*, 2011, **44**, 1339–1348.
10 C. J. Robinson, H. A. Vincent, M.-C. Wu, P. T. Lowe, M. S. Dunstan, D. Leys and J. Micklefield, *J. Am. Chem. Soc.*, 2014, **136**, 10615–10624.
11 P. Ceres, A. D. Garst, J. G. Marcano-Velázquez and R. T. Batey, *ACS Synth. Biol.*, 2013, **2**, 463–472.
12 E. Ennifar, P. Walter, B. Ehresmann, C. Ehresmann and P. Dumas, *Nat. Struct. Mol. Biol.*, 2001, **8**, 1064–1068.
13 F. Ducongé and J.-J. Toulmé, *RNA*, 1999, **5**, 1605–1614.
14 G. Durand, S. Lisi, C. Ravelet, E. Dausse, E. Peyrin and J.-J. Toulmé, *Angew. Chem., Int. Ed.*, 2014, **53**, 6942–6945.
15 K. Zhang, K. Wang, X. Zhu, M. Xie and F. Xu, *RSC Adv.*, 2016, **6**, 99269–99273.
16 K. Zhang, K. Wang, X. Zhu and M. Xie, *Biosens. Bioelectron.*, 2016, **78**, 154–159.
17 E. Engvall and P. Perlmann, *Immunochemistry*, 1971, **8**, 871–874.
18 Y. Cui, K. Liu, C. Xu, F. Liu, Q. X. Li, S. Liu and B. Wang, *Food Chem.*, 2014, **143**, 293–299.
19 M. F. Clark and A. N. Adams, *J. Gen. Virol.*, 1977, **34**, 475–483.
20 X. Bi and Z. Liu, *Anal. Chem.*, 2014, **86**, 959–966.
21 B. Berg, B. Cortazar, D. Tseng, H. Ozkan, S. Feng, Q. Wei, R. Y.-L. Chan, J. Burbano, Q. Farooqui, M. Lewinski, D. Di Carlo, O. B. Garner and A. Ozcan, *ACS Nano*, 2015, **9**, 7857–7866.
22 L. Asensio, I. Gonzalez, T. Garcia and R. Martin, *Food Control*, 2008, **19**, 1–8.
23 A. Apilux, Y. Ukita, M. Chikae, O. Chailapakul and Y. Takamura, *Lab Chip*, 2013, **13**, 126–135.
24 C.-H. Lai, L.-L. Chang, J.-N. Lin, W.-F. Chen, L.-L. Kuo, H.-H. Lin and Y.-H. Chen, *PLoS One*, 2013, **8**, e77640.
25 W. Jiang, Z. Wang, R. C. Beier, H. Jiang, Y. Wu and J. Shen, *Anal. Chem.*, 2013, **85**, 1995–1999.
26 X. Hua, J. Yang, L. Wang, Q. Fang, G. Zhang and F. Liu, *PLoS One*, 2012, **7**, e53099.
27 M. L. Hammock, O. Knopfmacher, T. N. Ng, J. B. H. Tok and Z. Bao, *Adv. Mater.*, 2014, **26**, 6138–6144.
28 K. Eyer, S. Stratz, P. Kuhn, S. K. Kuester and P. S. Dittrich, *Anal. Chem.*, 2013, **85**, 3280–3287.
29 E. Engvall and P. Perlmann, *J. Immunol.*, 1972, **109**, 129–135.
30 D. M. Rissin, C. W. Kan, T. G. Campbell, S. C. Howes, D. R. Fournier, L. Song, T. Piech, P. P. Patel, L. Chang, A. J. Rivnak, E. P. Ferrell, J. D. Randall, G. K. Provuncher, D. R. Walt and D. C. Duffy, *Nat. Biotechnol.*, 2010, **28**, 595–599.
31 D. Peng, L. Feng, Y. Pan, Y. Wang, D. Chen, J. Wang and Z. Yuan, *Food Chem.*, 2016, **197**, 821–828.
32 B.-H. Liu, Y.-T. Hsu, C.-C. Lu and F.-Y. Yu, *Food Control*, 2013, **30**, 184–189.
33 H. Lin, Y. Liu, J. Huo, A. Zhang, Y. Pan, H. Bai, Z. Jiao, T. Fang, X. Wang, Y. Cai, Q. Wang, Y. Zhang and X. Qian, *Anal. Chem.*, 2013, **85**, 6228–6232.
34 J. Liang, H. Liu, C. Huang, C. Yao, Q. Fu, X. Li, D. Cao, Z. Luo and Y. Tang, *Anal. Chem.*, 2015, **87**, 5790–5796.
35 H. Li, X. Yan, H. Shi and X. Yang, *Food Chem.*, 2014, **164**, 166–172.
36 R. M. Lequin, *Clin. Chem.*, 2005, **51**, 2415–2418.
37 W. Zhang, L. He, R. Zhang, S. Guo, H. Yue, X. Ning, G. Tan, Q. X. Li and B. Wang, *Food Chem.*, 2016, **207**, 233–238.
38 T.-T. Xiao, X.-Z. Shi, H.-F. Jiao, A.-L. Sun, H. Ding, R.-R. Zhang, D.-D. Pan, D.-X. Li and J. Chen, *Biosens. Bioelectron.*, 2016, **75**, 34–40.
39 Z. Wang, T. Mi, R. C. Beier, H. Zhang, Y. Sheng, W. Shi, S. Zhang and J. Shen, *Food Chem.*, 2015, **171**, 98–107.
40 S. Y. Toh, M. Citartan, S. C. B. Gopinath and T.-H. Tang, *Biosens. Bioelectron.*, 2015, **64**, 392–403.
41 S. Santiago-Felipe, L. A. Tortajada-Genaro, R. Puchades and A. Maquieira, *Anal. Chim. Acta*, 2014, **811**, 81–87.
42 Y. Huang, H. Li, Y. Zhang, W. Li, L. Sun and G. Li, *Chem. Commun.*, 2015, **51**, 11004–11007.
43 K. Zhang, K. Wang, X. Zhu, Y. Gao and M. Xie, *Chem. Commun.*, 2014, **50**, 14221–14224.
44 K. Zhang, T. Ren, K. Wang, X. Zhu, H. Wu and M. Xie, *Chem. Commun.*, 2014, **50**, 13342–13345.